

# Multiphase Flow-Related Defects in Continuous Casting of Steel Slabs



Seong-Mook Cho, Mingyi Liang, Hamed Olia, Lipsa Das  
and Brian G. Thomas

**Abstract** Multiphase flow phenomena greatly affect the quality of continuous cast steel. Air aspiration through a nozzle, due to negative pressure distribution, can cause reoxidation and non-metallic inclusions, which may build up on the refractory walls as nozzle clogging. Asymmetric jet flow from a clogged nozzle causes excessive surface velocities and vortexing at the top surface in the mold, resulting in entrainment of the mold slag into the steel pool. In addition, instability at the interface between the molten steel and surface slag, caused by jet wobbling, results in sudden level drops and slag entrapment into the solidifying shell at the meniscus region. This surface defect formation becomes more severe with meniscus freezing and the accompanying formation of subsurface hooks. Furthermore, particles such as argon gas bubbles, alumina inclusions, and entrained slag droplets can be transported deep into the strand and captured into the steel shell, especially on the inside radius wall during curved strand casting. This causes internal defects. To quantify the above defect formation mechanisms relevant to multiphase flow phenomena, high-resolution multiphase flow models validated with plant measurements and/or laboratory-scale model experiments are required. Finally, these multiphase flow-related defects can be lessened with appropriate choice of nozzle geometry and all of the casting conditions which control the flow. The specific effects of nozzle port angle, nozzle submergence depth, casting speed, gas injection, and electromagnetic forces are discussed.

**Keywords** Continuous caster · Argon bubble · Alumina · Aspiration · Clogging · Slag · Entrainment · Entrapment

---

S.-M. Cho · M. Liang · H. Olia · L. Das · B. G. Thomas (✉)  
Department of Mechanical Engineering, Colorado School of Mines, Brown Hall W470I, 1610  
Illinois Street, Golden, CO 80401, USA  
e-mail: [bgthomas@mines.edu](mailto:bgthomas@mines.edu)

S.-M. Cho  
e-mail: [seongmookcho1@mines.edu](mailto:seongmookcho1@mines.edu)

© The Minerals, Metals & Materials Society 2020  
The Minerals, Metals & Materials Society (ed.), *TMS 2020 149th  
Annual Meeting & Exhibition Supplemental Proceedings*, The Minerals,  
Metals & Materials Series, [https://doi.org/10.1007/978-3-030-36296-6\\_108](https://doi.org/10.1007/978-3-030-36296-6_108)

1161

## Introduction

Many defects including both surface and internal defects in final steel products are associated with complex multiphase flow phenomena, including molten steel-argon gas flow, transport of particles including non-metallic inclusions and argon gas bubbles, nozzle clogging, slag entrainment and entrapment, meniscus freezing, and particle capture into the solidifying steel shell during continuous casting.

Argon gas is injected into the molten steel to prevent the nozzle clogging. However, unoptimized injection conditions can produce undesirable mold flow, such as single roll flow or unstable flow patterns which are detrimental to the top surface flow, level, and defect formation [1]. Alumina inclusions flow into the casting mold through the nozzle from upstream processes, such as steel making, ladle refining, and tundish operations [2]. In addition, air aspiration increases alumina inclusions due to reoxidation of the alloys melted in the molten steel, leading to the nozzle clogging with heavy buildup of the inclusions at the nozzle wall [3]. A major cause of reoxidation is negative pressure inside the nozzle, which draws in air from the surroundings [3]. Clogging causes asymmetric internal shape of the nozzle bore and/or ports which can produce asymmetric flow in the mold during casting. This can lead to asymmetric and unstable flow across the top surface, causing excessive velocity and vortexing [4]. This in turn can lead to both slag entrainment into the molten steel pool [5, 6] and the entrapment of inclusions during initial solidification, which is especially detrimental to the surface quality of steel when there are also meniscus freezing and hook problems [7].

Particles including alumina inclusions, entrained slag droplets, and argon gas bubbles can be transported to the steel shell front, where they may be captured into the solidifying shell [8]. Those captured particles become defects in the final cast steel, if the surface layer oxidized away by subsequent scale formation and scarfing processes are insufficient to remove them. Subsequent rolling operations elongate these captured particles in the casting direction. The resulting sliver defects cause cracks and tearing during subsequent processes such as pressing, as shown in Fig. 1a. Scab defects (Fig. 1b) associated with slag entrainment and entrapment appear with non-uniform shapes mostly on plate edge regions. Captured bubbles may expand the surface during annealing processes, and/ or elongate during pressing, leading to



**Fig. 1** Example defects on final steel products: **a** sliver [9], **b** scab [10], and **c** blister defects [9]

expensive blister defects on the surface of final steel products [2], such as shown in Fig. 1c.

This paper briefly introduces various tools to quantify the multiphase flow phenomena related to defect formation in continuous steel casting. Then, defect formation mechanisms related to multiphase flow are reviewed, such as air aspiration and nozzle clogging, slag entrainment, particle entrapment including surface capture (slag entrapment and meniscus freezing) and internal capture. Examples include multiphase flow simulation, water model experiments, and plant measurements. Finally, some practical strategies to control multiphase flow-related defects are discussed.

## Tools to Quantify Defect Formation Mechanisms

To quantify multiphase flow phenomena and the associated defects, computational modeling, laboratory-scale modeling, and plant measurements have been widely used, as reviewed previously [11]. Each method has both merits and limitations. It is best to apply computational models validated with measurements in laboratory models and/or real plant.

Multiphase computational fluid dynamics (CFD) models include volume of fluid (VOF) for slag/steel interfacial motion, mixture and Eulerian–Eulerian (EE) models for molten steel-argon gas flow, Lagrangian discrete phase model (DPM) for particle trajectory, and the hybrid model, EEDPM for argon bubble interaction, particle capture models for particle entrapment between primary dendrite arm spacing (PDAS) and/or by subsurface hooks, as reviewed previously [12, 13].

Laboratory-scale models using water or a low melting alloy are also a useful tool, especially if similarity between the model and the real caster can be obtained. Matching both Froude number and Weber number is important to simulate multiphase flow phenomena, especially with high gas flow rates and volume fractions. This can be achieved with a 0.6 scale model [2, 14].

Plant measurements include nail dipping tests for surface velocity and level, and oscillation mark measurements for initial solidification, and surface profile variations. Particle capture measurements in as-cast slabs and billets include ultrasonic testing, step milling followed by visual or microscopy measurements, and other methods reviewed previously [15]. Finally, it is important to observe and quantify the real defects found in the final products.

## Air Aspiration and Nozzle Clogging

The pressure distribution inside the nozzle during continuous steel casting is important to steel quality. Figure 2 shows the vertical pressure distribution inside a nozzle with a slide gate, predicted from both a three-dimensional EE model simulation of

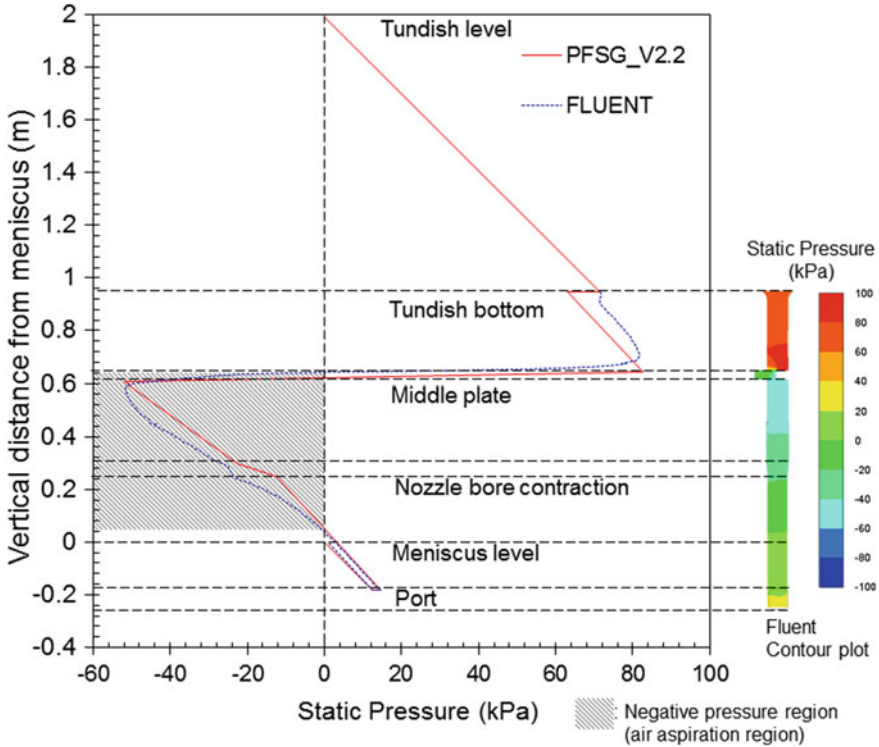


**Fig. 2** Pressure distribution inside a nozzle with a slide gate comparing CFD prediction and PFSG calculation [18]

molten steel-argon gas flow with FLUENT [16] and a one-dimensional pressure-energy model calculation using the pressure-drop flow-rate model for slide gate systems program (PFSG) [17]. Both model predictions match reasonably and reveal a large negative pressure region from the middle plate to the meniscus. The negative pressure is generated by sudden contraction of the nozzle bore due to the reduced area of the slide-gate opening, which controls molten steel flow rate during continuous casting. The negative pressure region indicates possible air aspiration region, resulting in reoxidation and oxide inclusions. Buildup of these inclusions on the nozzle walls often leads to nozzle clogging, shown in Fig. 3, especially in regions such as near the slide gate and/or the upper region of nozzle ports, where the flow is relatively stagnant due to recirculation.

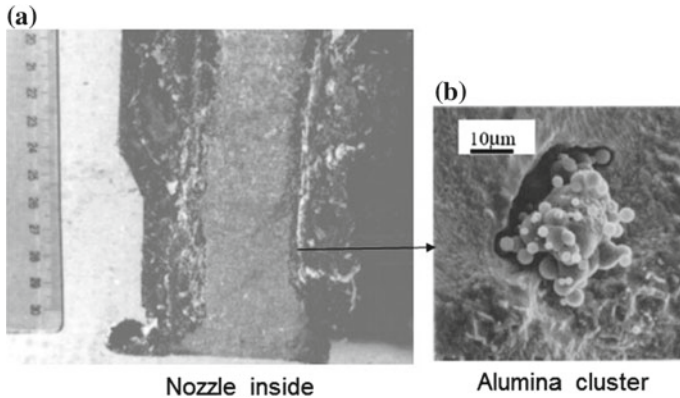


Fig. 3 a Nozzle clogging [19] and b alumina cluster in the clog [20]

### Slag Entrainment

Mold powder is added to the top of the molten steel pool, where it melts to form a slag layer which protects the steel from reoxidation, lubricates the gap between the solidifying steel shell and mold walls, and hopefully traps any non-metallic inclusions and bubbles coated with inclusions [21] which reach the top surface during casting. However, the surface slag can be entrained into the steel pool, due to various mechanisms [6] shown in Fig. 4. The most important mechanism(s) depend on casting conditions, and several mechanisms often combine together. Surface defects are often due mainly to surface-level fluctuations, meniscus freezing, hook formation, and surface wave instability. Internal defects often arise from vortex formation, shear layer instability, upward flow, argon bubble interactions/slag foaming, slag crawling, and surface balding. Slag droplets entrained by these mechanisms lead to defects

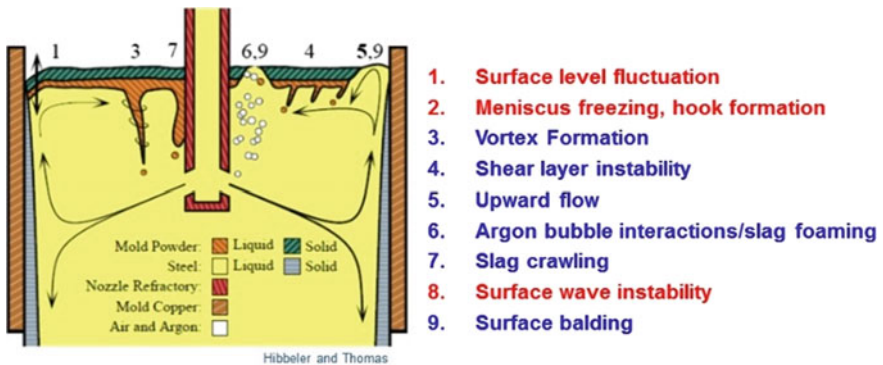
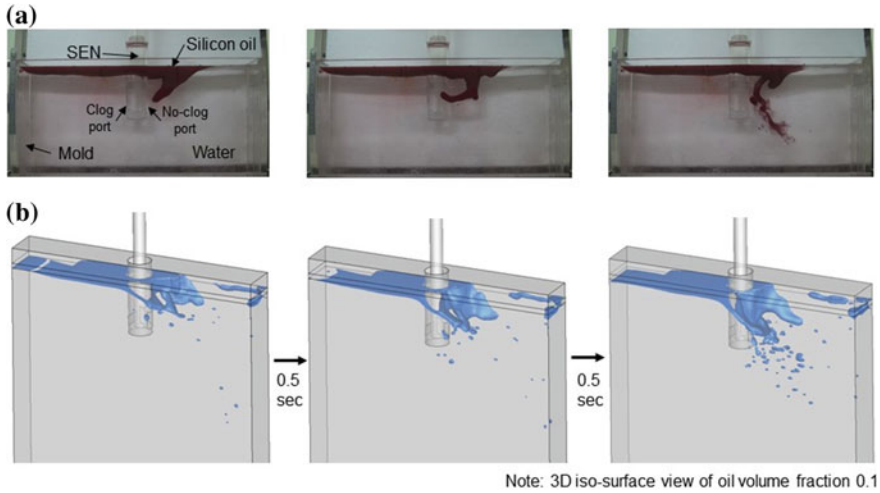


Fig. 4 Slag entrainment mechanisms in a continuous casting mold [6]



**Fig. 5** Slag entrainment in a mold with a clogged nozzle during continuous steel-slab casting, observed in **a** 1/3-scale water-oil model experiments and simulated by **b** LES-VOF modeling of the water model [5]

when they become entrapped into the steel shell deep in the strand. Furthermore, they all have both quasi-steady and transient aspects.

Figure 5 shows shear layer and shear wave instability slag entrainment mechanisms in 1/3 scale water model experiments with silicon oil. In this example, nozzle port clogging causes slag entrainment from the interface between the surface slag (oil) and molten steel pool (water) on the side of the mold with the non-clogged port. Surface flow later drags the slag fingers into the molten steel pool, where they break up into entrained droplets.

## Particle Entrapment

Particles including alumina inclusions, entrained slag droplets, and argon gas bubbles are transported by the mold flow and will lead to defects if they are unable to be safely removed into the top surface slag, and become entrapped into the steel shell. Some particles are entrapped near the meniscus due to surface-level fluctuations, and/or by meniscus freezing, causing surface defects. Alternatively, the mold flow transports particles to near the solidifying steel shell front, where they may be entrapped by the steel shell. If the entrapment is lower down the strand, they end up as internal defects.

### Surface-Level Fluctuations and Slag Entrapment

The jets from different angles of nozzle ports generate different flow patterns and liquid mold flux behavior in the mold, as shown for example in Fig. 6. As shown in Fig. 6a, a finger-like protrusion from the liquid slag layer is observed near where the jet impinges on the top surface. Jet wobbling due to an unstable flow pattern associated with the upward nozzle port (Fig. 6a) produces transient variations in the impingement point on the top surface, leading to this entrainment phenomenon [10]. Flow variations inside the nozzle are another way that jet wobbling, velocity variations, level fluctuations, and defects can occur.

Slag entrained near the meniscus can be directly entrapped into the initial solidification front. Figure 7 shows an instantaneous surface slag/molten steel interface

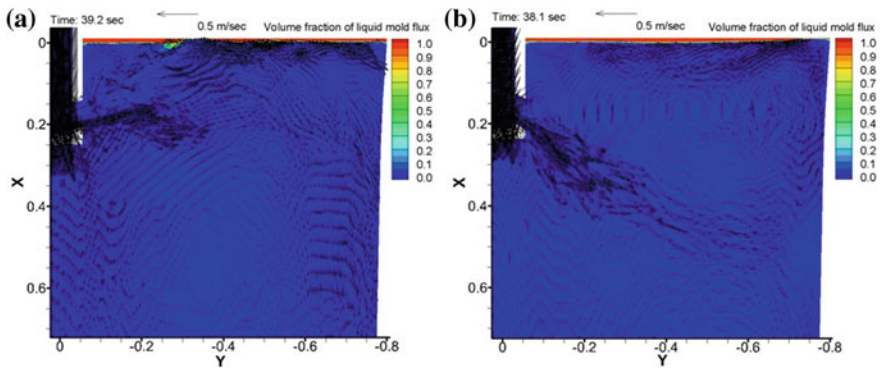


Fig. 6 Instantaneous slag/steel interface behavior in a slab casting mold with **a** upward-angled ports and **b** downward-angled ports [10]

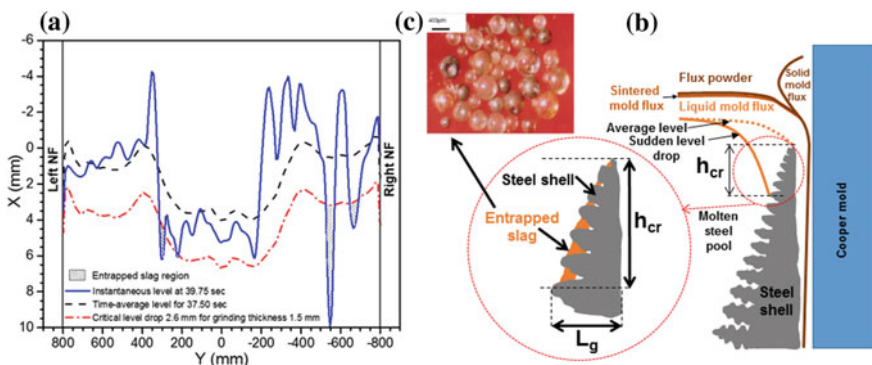


Fig. 7 **a** LES modeling of slag entrapment into solidifying steel shell on IR, due to sudden level drops, **b** schematic of the slag entrapment mechanism [10], and **c** entrapped spherical slag inclusions [15]



predicted from the LES-VOF simulation shown in Fig. 6a and potential slag entrainment regions near the meniscus. The surface level drops over 10 mm relative to the time-average level, which can produce an 8 mm vertical length of slag entrainment. Such entrapped slag can become a surface defect if the slag is unable to be removed during scale formation or subsequent scarfing processes.

### *Meniscus Freezing and Surface Defects*

Superheat is transported by the fluid flow in the continuous casting mold. Unoptimized mold flow may lead to slow-flowing regions, low superheat, near the meniscus region, causing the meniscus freezing. This leads to abnormal initial solidification structures, called hooks in the subsurface region as shown in Fig. 8. The deeper hooks near the corner region are more detrimental to steel surface quality because they can easily capture particles such as argon bubbles coated with inclusions, slag droplets, or slag/ bubble mixtures (foam) [22]. These particles should be removed into the surface slag due to their buoyancy, but the deep hooks may trap them and prevent their reaching at the surface. Alternatively, other slag entrainment mechanisms, such as level fluctuations previously explained, become more severe when hooks are present, which results in more surface defects.

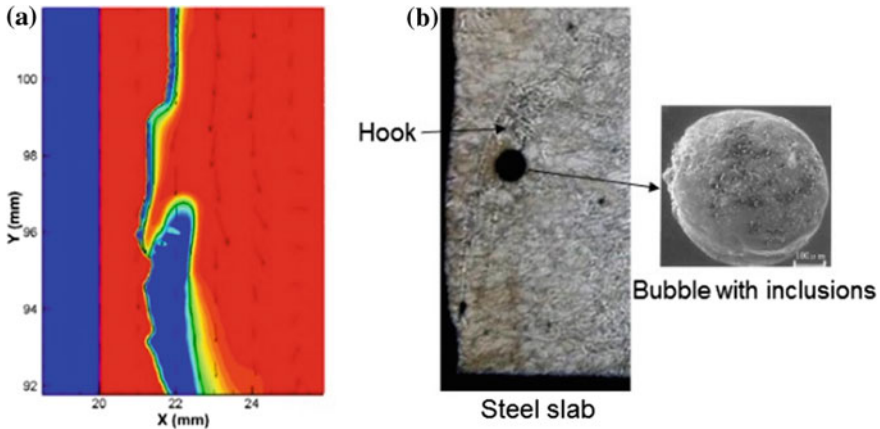


**Fig. 8** **a** Meniscus region freezing (simulation) [23] and **b** bubble coated with inclusions [24] captured by a subsurface hook



### Internal Particle Capture

Particles delivered deep into the strand can be detrimental to internal steel quality if they are entrapped by the solidifying steel shell: either by entering between the primary dendrite arms, or by balancing at the front while they become surrounded by the growing dendrites. These particles become internal defects.

Figure 9 shows the flow patterns and the argon bubble capture locations in a typical strand caster that has a curved region starting below an upper straight region that includes the mold. A large recirculation region (over 2 m long) with flow stagnation is generated near the straight/curved transition region, as shown in the side views taken at the quarter vertical plane (0.58 m from the strand center). This flow recirculation is likely due to bubble buoyancy causing rising flow in the relatively stagnant region near the inside radius shell. Strong downward flow from the jets impinging on the narrow faces tends to extend straight down near the outside radius shell. More particles are captured at the stagnant or upward flowing regions: the straight/curved transition on IR or deeper in the strand.

Finally, the entrapped particles remain in the solidified steel slab, as shown in end view of the strand (Fig. 10; note: the colored dots (predicted from the particle capture simulation) and the black dots (measured from the UT measurements) show the locations of captured particles). Most captured particles are observed near the straight/curved transition region (green dash line), as also shown in Fig. 9. These particles are detrimental to the quality of final steel products after later processing. Especially, the captured bubbles expand during annealing processes and then elongate during rolling processes, resulting in pencil pipe blister defects on the final steel product, as shown in Fig. 11. These defects are very expensive because often they

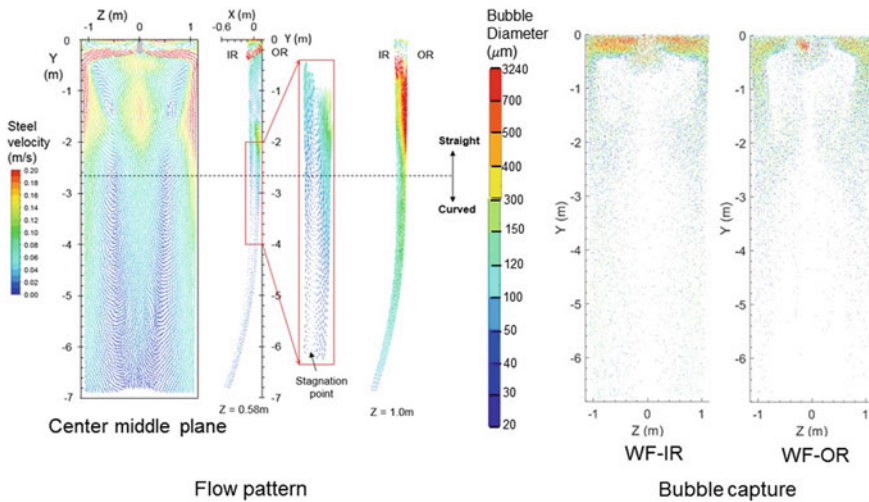
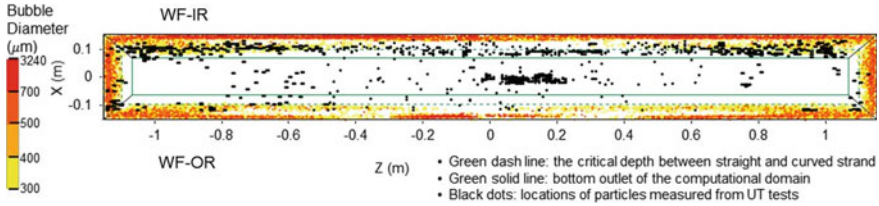
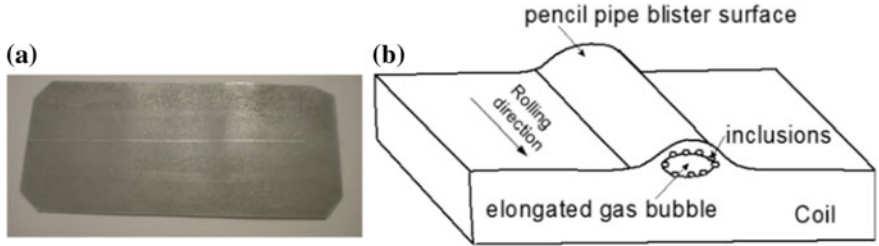


Fig. 9 Flow pattern and bubble capture distribution in curved strand casting [18]



**Fig. 10** End view of steel slab comparing predicted particle capture locations with UT measurements [18]



**Fig. 11** Pencil pipe blister defect: **a** observed at a steel coil surface and **b** described inside the coil [25]

are not detected after the final product has been painted, when differences in light reflection from the blistered surface can be observed.

### Control of Defect Formation

To reduce the defects related to multiphase flow phenomena in continuous steel casting, caster geometry (nozzle port angle, size, and shape, mold width and thickness, etc) and process conditions (casting speed, argon gas injection, nozzle submergence depth, electromagnetic forces) must be controlled together within windows of safe process operation [1]. High-quality steel products depend on finding combinations of process parameters which generate surface flows which are simultaneously slow enough to avoid slag entrainment defects due to surface instability, and fast enough to ensure sufficient superheat transport to avoid surface defects due to meniscus freezing.

Nozzle geometry including size, shape, and especially port angle, strongly influences the mold flow pattern and its stability [26]. The downward nozzle ports shown in Fig. 6b avoid the surface impingement, level fluctuations, slag entrainment, and associated defects of the upward nozzle ports in Fig. 6a, for the other flow conditions of this example [10].

The SEN submergence depth is an influential parameter on flow pattern [27]. Adjusting SEN submergence according to other process conditions (especially the casting speed and mold width) has the potential to maintain the surface velocity within an acceptable range to avoid slag entrainment due to excessive velocity and surface defects due to meniscus freezing from insufficient surface velocity.

Finally, the application of electromagnetic forces is both highly influential on the flow pattern and relatively easy to change during operation. In addition, these forces intrinsically adjust to turbulent variations in the molten steel flow. Thus, the use of electromagnetic forces is an attractive method to control the flow pattern, especially for casting conditions prone to unstable flow, such as large strand width, and/or high casting speed. For example, with double-ruler EMBR, positioning the upper field just above the jet and the lower field just below the jet [28, 29] can continuously deflect the jet to lessen surface velocity variations and level fluctuations, especially for high-speed casting [11]. To achieve the benefits, it is very important to understand the relevant defect formation mechanisms and how the electromagnetic forces interact with the other casting parameters to control the flow pattern and those mechanisms.

## Summary and Conclusions

This paper illustrates several mechanisms of multiphase flow-related defects in continuous steel casting, quantified by applying various tools including multiphase CFD models, laboratory-scale water models, and plant measurements. In addition, practical strategies to control defects are discussed. Some important conclusions are summarized below:

- High-resolution multiphase flow modeling validated with measurements using water models and/or a real plant is best to accurately quantify the mechanisms of multiphase flow-related defect formation.
- Air aspirated into the nozzle due to negative pressure produces non-metallic inclusions, leading to buildup of the inclusions on the nozzle walls and nozzle clogging. This can cause asymmetric mold flow and vortex formation, and excessive surface velocity and level fluctuations, leading to slag entrainment defects.
- Surface slag can be entrained due to several (9) interacting mechanisms. Entrained slag droplets and other particles can be captured into the solidifying shell, leading to surface defects if entrapped near the meniscus, or internal defects, if entrapped deeper.
- Surface-level fluctuations can cause both slag entrainment and particle entrapment near the meniscus region, leading to surface defects.
- Insufficient surface flows lead to lower local superheat and freezing of the meniscus region, leading to defects due to deep hook structures.
- Particles captured between the primary dendrite arms or surrounded by the growing dendrites can become defects if they are not close enough to the surface to be removed by scale formation or scarfing processes.

- The inside radius near the straight/curved transition of the caster is more prone to capture large particles, because a flow recirculation region is generated there, which makes velocities near the inside radius solidification front become stagnant and thus makes particle entrapment easier.
- Reducing defects needs comprehensive management of all of the influential process parameters that affect flow in order to control multiphase flow phenomena within a safe range for high-quality steel, based on good quantitative understanding of the competing and complex defect formation mechanisms.

**Acknowledgements** Support from the Continuous Casting Center at Colorado School of Mines, the Continuous Casting Consortium at University of Illinois at Urbana-Champaign, POSCO, South Korea (Grant No. 4.0011721.01), and the National Science Foundation GOALI grant (Grant No. CMMI 18-08731) is gratefully acknowledged. Provision of FLUENT licenses through the ANSYS Inc. academic partnership program is also much appreciated. This research is part of the Blue Waters sustained-petascale computing project, which is supported by the National Science Foundation (awards OCI-0725070 and ACI-1238993) and the state of Illinois. Blue Waters is a joint effort of the University of Illinois at Urbana-Champaign and its National Center for Supercomputing Applications.

## References

1. Dauby PH (2012) Continuous casting: make better steel and more of it! *Revue de Métallurgie* 109:113–136
2. Zhang L, Yang S, Cai K, Li J, Wan X, Thomas BG (2007) Investigation of fluid flow and steel cleanliness in the continuous casting strand. *Metall Mater Trans B* 38(1):63–83
3. Rackers K, Thomas BG (1995) Clogging in continuous casting tundish nozzle. In: Paper presented at the 78th steelmaking conference, Nashville, TN, USA, 2 April 1995
4. Cho S-M, Kim S-H, Chaudhary R, Thomas BG, Shin H-J, Choi W-Y, Kim S-K (2012) Effect of nozzle clogging on surface flow and vortex formation in the continuous casting mold. *Iron Steel Technol* 9(7):85–95
5. Cho S-M, Thomas BG, Kim S-H, Lee H-J (2015) Investigation of flow pattern, surface behavior, and mold slag entrainment using oil-water model, CFD model, and plant test. In: Presented at the CCC annual meeting, Champaign, IL, USA, 19 August 2015
6. Hibbeler LC, Thomas BG (2013) Mold slag entrainment mechanisms in continuous casting molds. *Iron Steel Technol* 10:121–134
7. Shin H-J, Kim S-H, Thomas BG, Lee G-G, Park J-M, Sengupta J (2006) Measurement and prediction of lubrication, powder consumption, and oscillation mark profiles in ultra-low carbon steel slabs. *ISIJ Int* 46:1635–1644
8. Thomas BG, Yuan Q, Mahmood S, Liu R, Chaudhary R (2014) Transport and entrapment of particles in steel continuous casting. *Metall Mater Trans B* 45(1):22–35
9. Lee G-G, Thomas BG (2007) Multi-phase asymmetric fluid flow and inclusion entrapment in the slab mold. In: Presented at the CCC annual meeting, Champaign, IL, USA, 12 June 2007
10. Cho S-M, Thomas BG, Kim S-H (2019) Effect of nozzle port angle on transient flow and surface slag behavior during continuous steel-slab casting. *Metall Mater Trans B* 50(1):52–76
11. Cho S-M, Thomas BG (2019) Electromagnetic forces in continuous casting of steel slabs. *Metals (Special Issue: Continuous Casting)* 9:471 (1–38)
12. Yang H, Vanka SP, Thomas BG (2019) Mathematical modeling of multiphase flow in steel continuous casting. *ISIJ Int* 56(6):956–972

13. Thomas BG (2018) Review on modeling and simulation of continuous casting. *Steel Res Int* 89:1700312 (1–21)
14. Singh PK, Mazumdar D (2019) Mathematical modelling of gas-liquid, two-phase flows in a ladle shroud. *Metall Mater Trans B* 50(2):1091–1103
15. Zhang L, Thomas BG (2003) State of the art in evaluation and control of steel cleanliness. *ISIJ Int* 43:271–291
16. ANSYS FLUENT 14.5-Theory Guide, ANSYS, Inc., Canonsburg, PA, USA (2012)
17. Olia H, Thomas BG (2018) PFSG (Pressure drop Flow rate for Slide Gate system) Manual Version 2.0. Manual presented at the CCC annual meeting, Golden, CO., USA, 15 August 2018
18. Liang M, Cho S-M, Olia H, Das L, Thomas BG (2019) Modeling of multiphase flow and argon bubble entrapment in continuous slab casting of steel. In: Paper presented at the AISTECH 2019, Pittsburgh, PA, USA, 6–9 May 2019
19. Rackers KG (1995) Mechanism and mitigation of clogging in continuous casting nozzles. M.S. Thesis, University of Illinois
20. Rege RA, Szekeres ES, Forgeng WD (1970) *Met Trans AIME* 1:2652
21. Zhang L, Aoki J, Thomas BG (2006) Inclusion removal by bubble floatation in a continuous casting mold. *Metall Mater Trans B* 37(3):361–379
22. Emling WH, Waugaman TA, Feldbauer SL, Cramb AW (1994) Subsurface mold slag entrainment in ultralow carbon steels. In: Paper presented at the 77 steelmaking conference, Chicago, IL, USA, 20–23 March 1994
23. Yan X, Jonayat A, Thomas BG (2016) Thermal-fluid model of meniscus behavior during mold oscillation in steel continuous casting, CCC report
24. Miki Y, Takeuchi S (2003) *Iron Steel Inst Jpn* 43:1548–1555
25. Thomas BG (2019) Nozzle design and flow issues in slab casting. In: Presented at the Brimacombe continuous casting short course, Vancouver, B.C., Canada, 1–5 April 2019
26. Najjar FM, Thomas BG, Hershey DE (1995) Numerical study of steady turbulent flow through bifurcated nozzles in continuous casting. *Metall Mater Trans B* 26:749–765
27. Jin K, Vanka SP, Thomas BG (2017) Large eddy simulations of the effects of EMBr and SEN submergence depth on turbulent flow in the mold region of a steel caster. *Metall Mater Trans B* 48(1):162–178
28. Cho S-M, Thomas BG, Kim S-H (2016) Transient two-phase flow in slide-gate nozzle and mold of continuous steel slab casting with and without double-ruler electro-magnetic braking. *Metall Mater Trans B* 47(5):3080–3098
29. Jin K, Vanka SP, Thomas BG (2018) Large eddy simulations of electromagnetic braking effects on argon bubble transport and capture in a steel continuous casting mold. *Metall Mater Trans B* 49(3):1360–1377